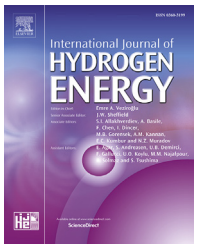
Available online at www.sciencedirect.com

ScienceDirect

journal homepage: www.elsevier.com/locate/he



Investigations on performance and emission characteristics of an industrial low swirl burner while burning natural gas, methane, hydrogen-enriched natural gas and hydrogen as fuels

Mehmet Salih Cellek[*], *Ali Pınarbaşı*

Heat and Thermodynamics Division, Department of Mechanical Engineering, Mechanical Engineering Faculty, Yildiz Technical University, Yildiz, Besiktas, Istanbul 34349, Turkey

ARTICLE INFO

Article history:
Received 9 March 2017
Received in revised form
24 April 2017
Accepted 14 May 2017
Available online 9 June 2017

Keywords:
LSB
Natural gas
Methane
Hydrogen
Hydrogen-enriched
Eddy Dissipation method

ABSTRACT

Although many detailed chemical reaction mechanisms, skeletal mechanisms and reduced mechanisms are available in the literature to modeling the natural gas, they are computational expensive, required high power computing especially for three dimensional complex geometries with intense meshes. For example, though the DRM19 reduced mechanism does not include NO and NO_2 species, it includes 19 species and 84 reactions. On the other hand, Eddy Dissipation combustion model in which the overall rate of reaction is mainly controlled by turbulent mixing can be utilized as a practical approach for fast burning and fast reaction fuels such as natural gas. Unlike fossil fuels, hydrogen is a renewable energy and quite clean in terms of carbon monoxide and carbon dioxide emissions. However, numerical and experimental studies on hydrogen combustion in burners are very restricted. In this study, the combustion of natural gas in an industrial low swirl burner–boiler system has been experimentally investigated. The results obtained from the experimental setup have been utilized as boundary conditions for CFD simulations. With the use of Eddy Dissipation method, methane-air-2-step reaction mechanism is used for modeling of natural gas as methane gas and the reaction mechanism has been modified for natural gas considering the natural gas properties to reveal the similarities and differences of both fuels in modeling. In addition, the combustion performances of natural gas with the use of full and periodic models, which are geometric models of the burner–boiler pair, are compared. Moreover, in order to reveal the effect of the hydrogen-enriched natural gas and pure hydrogen on the performance of low swirl burner–boiler considering the combustion emissions, four various gas contents (thermal load ratio: 75% NG + 25%H_2, 50%NG + 50%H_2, 25%NG + 75%H_2, 100%H_2) at the same thermal load have been investigated. The turbulent flames of the industrial low swirl burner have been studied numerically using ANSYS Fluent 16.0 for the solution of governing equations. The results obtained in this study show that with the utilizing Eddy Dissipation method, natural gas can be modeled as methane gas with well-known methane-air-2step reaction mechanism or as natural gas with modified methane-air-2step reaction mechanism with approximate results. Additionally, the use of periodic boundary condition, which enables

* *Corresponding author.*
E-mail addresses: mscellek@gmail.com, alipnrbs@yildiz.edu.tr (M.S. Cellek).
http://dx.doi.org/10.1016/j.ijhydene.2017.05.107
0360-3199/© 2017 Hydrogen Energy Publications LLC. Published by Elsevier Ltd. All rights reserved.

studying with 1/4 of geometric model, gives satisfactory results with less number of meshes when compared to the full model. Furthermore, in the case of using hydrogen-enriched natural gas or pure hydrogen instead of natural gas as the fuel, the combustion emissions of the burner–boiler such as CO and CO_2 are remarkably decreasing compared to the natural gas. However, the NOx emissions are significantly increasing especially due to thermal NO.

© 2017 Hydrogen Energy Publications LLC. Published by Elsevier Ltd. All rights reserved.

Introduction

On one hand, the combustion emissions of fossil fuels and their atmospheric damage continue to increase, on the other hand, the gradual depletion of fossil fuels such as coal, crude oil and natural gas has become one of the most worrisome and controversial issues of our time.

The use of carbon based fuels such as carbon dioxide (CO_2) and carbon monoxide (CO) lead to continuous increase in the emissions of greenhouse gases. While the impact of the CO_2 on global warming is significant, the effect of CO is very low. However the CO has significant indirect effects. Namely, it reacts with OH radicals in the atmosphere, and decreases the amount of them. Since OH radicals behave as an inhibitor to diminish the strong greenhouse gases such as methane. In addition, CO is able to spearhead the formation of the tropospheric greenhouse gas 'ozone' [1]. Therefore, environmentally friendly, new alternative energy sources are needed.

By the way, hydrogen is a renewable synthetic fuel that has recently attracted attention and required more field-tested, and can be used as an alternative fuel for many areas. Unlike fossil fuels, due to containing only water vapor as combustion emission while burned with oxygen, hydrogen is known as environment friendly and zero emission future green fuel [2]. Therefore, the use of hydrogen fuel instead of carbon-based fuels can be considered as the most effective way to prevent hazardous emissions such as CO_2, CO, Sulphur oxide and organic acids [3–5] when faced up increasing power requirements [6].

The combustion of hydrogen in engines, burners and gas turbines forms also nitrogen oxides (NOx) together with water vapor as combustion products. However, hydrogen fuel cell vehicles (HFCV) do not produce air pollutants, they emit only water vapor and leaked hydrogen [7]. Besides, in the fuel cell the reaction between hydrogen and oxygen is very controlled and happens at much slower rate, however, the reaction is rapid and uncontrolled in the internal combustion engines [8]. The performance of the fuel cell system mainly rely on the pressure, stoichiometry and humidity, cell operation temperature, temperature of reactant of gases and geometry of the components [9].

Hydrogen can be produced with different methods such as reforming natural gas, partial oxidation of liquid fuels, gasification of coal or biomass [10] and using renewable resources. Additionally, a few methodologies in advances such as chemical, biological, electrolytic, photolytic and thermochemical can be utilized for its production [11,12]. Although the most significant problem to think hydrogen as a fuel is storage, many innovative research and advancement work are going on for recognizing the most economical and highly efficient storage routes such as compressed gas, cryogenic, metal hydrides, carbon nanotubes proposed by Sharma and Ghoshal [11].

By taking into consideration the progress of alternative fuels, hydrogen and hydrogen-blended hydrocarbon fuels are greatly draw attention by many researchers. Yilmaz and Ilbas experimentally investigated the effects of excess air ratio, thermal power and fuel composition on the combustion chamber using hydrogen–methane mixed fuels [13]. It was observed that the increase of hydrogen in fuel composition increases the overall chamber temperatures while increase of excess air decreases the corresponding temperatures. Thermal power was found to have no influence on the chamber temperatures. In the another study of the same authors [14], as an extension for their previous study, increase of hydrogen composition in fuel was found to reduce the CO emissions by lowering methane composition in fuel. NO emissions were also found to be lower than the pure hydrogen combustion case. Additionally, in their numerically investigated study [15], k–ε and P–I models are found to have the most successful results compared with experimental study for turbulence and radiation models respectively. Flame temperature was increased by adding hydrogen to the fuel. Hydrogen addition was also found to reduce CO_2 and increase H_2O amount in combustion gases as observed by the numerical results. Bouras et al. [16] investigated coupled models namely LES and PDF model that give satisfactory agreement with the experimental data for the reference case. In addition, it is stated that increasing amount of hydrogen in the methane affected the chemical and physical data of the reactive system. Furthermore, hydrogen addition in the fuel in the reactive mixture resulted in rising the temperature and velocity of the burning gases and decreasing the emission of CO gases. Haj Ayed et al. [17] studied the effect of burner design parameters and combustion models on flame structure, flow field and NOx emissions of micromix hydrogen combustion. A fuel injector with diameter of 0.3 mm was tested in micromix burner under atmospheric conditions for a low energy density. Numerically analyzed study showed that the flame structure and the level of NOx emission in hydrogen combustion helped to understand flow characteristics in order to reveal further burner performance optimization. Besides, Haj Ayed et al. [18] examined the effect of the different design parameters of the high energy density micromix burner having injector diameter of 1 mm on the NOx emission and flame structure numerically. The findings showed that while the micromix burner proofed its dry-low-NOx level while the

energy density increased. Increased energy density caused thicker and longer flame and higher temperature because of NO formation. Sandalcı and Karagöz [3] experimentally studied the effect of hydrogen energy fraction on indicated thermal efficiency, CO, CO_2 and smoke emissions by using a diesel engine which was operated with 1300 rpm constant engine speed and 5.1 kW constant indicated power. The results revealed that indicated thermal efficiency of the engine, indicated specific CO, CO_2 and smoke emissions decrease. However, the isfc and NOx values (for %36 and 46%, respectively) increase with an increasing hydrogen energy fraction. Moreover, it was observed that peak heat release rate rises with increasing hydrogen energy fraction. Coppens et al. [19] examined experimentally and computationally the determination of hydrogen enrichment from 0% to 35% in cellular premixed flames of $CH_4 + O_2 + CO_2$ and adiabatic flat on propagation speeds. Increasing of hydrogen content in fuel led to reduction of the mean cell diameter, increment of the cell number and increment of the laminar burning velocities. Schefer et al. [20] numerically analyzed the effects of hydrogen enrichment on methane with in a 45-degree lean premixed swirly burner. They presented that while increasing of hydrogen amount in a fuel by 13.8% led to raise OH concentration by 44% and the lean stability limit decreased with the hydrogen addition. Ouimette and Seers [21] studied the effects of five different fuels $H_2/CO/CO_2$ over a wide range of equivalence ratio for partially premixed laminar flames. The results show that the flame temperature and flame height are diminished with the addition of CO_2 however their change are less important with the ratio of H_2/CO. Additionally, the EINOx level is decreased with the addition of CO_2 for whole range of equivalence ratios. On the other hand, the EINOx level decreased only for $\Phi \leq 2.0$ with the increase in H_2/CO ratio. Moreover the flame appearance changes with the variation of H_2/CO and addition of CO_2. Dutka et al. [22] investigate emissions of NOx and characterises the turbulent flow field with partially premixed bluff body (PPBB) burner. The obtained results based on this study show that lance position relative to the burner throat influence the NOx and CO emissions. To decrease the burner lance position accelerate the air flow result in decreasing the NOx emissions but negatively affecting the flame stability and condition of combustion. Additionally, the NOx are increased with the presence of the secondary ports for CH_4 but the situation reverses for the H_2 combustion. Moreover, the NOx emissions increase with the increase in the temperature of the chamber for CH_4 and H_2.

Intensive experimental studies maintained by many researches for more specific combustion cases, on the other hand, recent development in computer technology such as workstation and high performance computing cluster, Computer Aided Design (CAD) and Computational Fluid Dynamics (CFD) lead to specific important facilities to design of any machines or investigate the complex and the high turbulence internal flows. CAD and CFD allow not only interpreting design procedure and the internal flow but also enable optimizing the product components with less cost and waste of time before the manufacturing stage [23].

It can be seen from the literature that hydrogen is a new alternative energy source and it is required more field-tested for evaluation potential usage in many area. Although there are several studies focused on the hydrogen combustion in gas turbine combustor, a few ones are related to specific burner combustion. In other words, the studies about hydrogen-enriched natural gas combustion especially for burner and boiler are very restricted in the literature. Therefore, this study contributes to this area. In additional revealing the advantage of the periodic model over the full model, the combustion characteristics of methane, natural gas, and pure hydrogen and hydrogen-enriched natural gas composite fuels have been investigated by means of ANSYS FLUENT 16 [24] in a low swirl burner–boiler combustion system.

Experimental test rig, fuels and uncertainties

In this study, the simulated burner and boiler were supplied by the company of Termo-Heat Isı San. A.Ş [25] which also produces the existing ECOSTAR labeled burner. In the experimental part of this study, only natural gas tests were carried out to validate CFD results. The experimental results obtained from the test results were used as boundary conditions for CFD analyzes that are the investigations on the effects of various fuels such as 100% of methane, 100% of natural gas, 100% of hydrogen and hydrogen–natural gas blending fuels (heat load ratio: 75% NG – 25% H_2, 50% NG – 50% H_2 and 25% NG – 75% H_2) at constant burner load (1085 kW) and under the same boiler cooling conditions. The emission levels (NOx, CO, CO_2) were utilized as performance indicators for the both experiments and numerical studies. The experimental test rig is presented in Fig. 1. Besides, utilized natural gas for both experimental tests and modeling are presented in Fig. 2. The properties of the studied fuels are shown in Table 1. Accuracies of the measurements and the uncertainties in the calculated results are shown in Table 2.

Geometrical model of the burner and boiler

The geometry of the burner and boiler considered for the numerical calculations for this study is based on the CAD



Fig. 1 – The experimental test rig installed in the company of Termo-Heat Isı San. A.Ş.

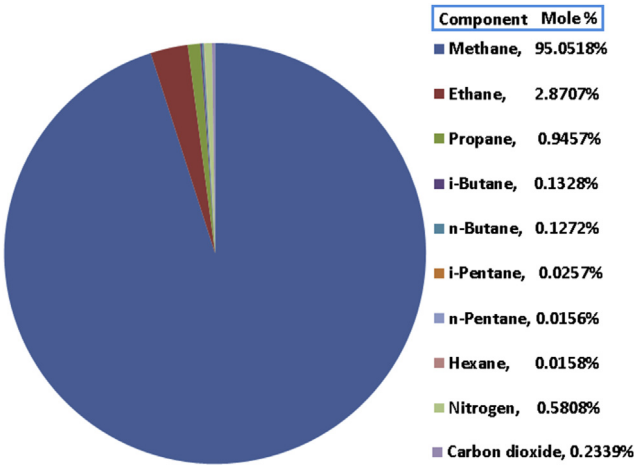


Fig. 2 – Components of natural gas [26] used in testing and numerical simulations.

Table 2 – Accuracies of the measurements and the uncertainties in the calculated results.

Measured parameter	Measurement devices	Range	Accuracy
$\dot{Q}$ gas	Sensyflow iG	Max. 6500 Nm^3/h	±0.3% Vol.
$\dot{Q}$ cooling water	ProcessMaster300	Max. 600 m^3/h	±0.4% Vol.
O_2	NOVA plus	0–21%	±0.2% Vol.
CO	NOVA plus	0–300 ppm	±2 ppm
CO	NOVA plus	0–4000 ppm	±100 ppm
CO_2	NOVA plus	0–3%	±0.5% Vol.
NO	NOVA plus	0–300 ppm	±2 ppm
NO	NOVA plus	0–1000 ppm	±5 ppm
NO_2	NOVA plus	0–200 ppm	±5 ppm
CH_4	NOVA plus	0–3%	±0.03%s
T_{air}	NOVA plus	0–100 °C	±1 °C
T_{smooke}	NOVA plus	0–650 °C	±2 °C
Calculated result			Uncertainty
Burner load			±0.3%
NOx			±7 ppm

modeling of ECO 45 GC 3b labeled ECOSTAR burner. An oxidizer and sufficient amount of heat is required to initiate the chemical reaction chain. Therefore, oxidizer air is fed into the boiler from outer annular side of the burner, whereas fuel is injected from inner side of the burner with the use of eight separated nozzles. A swirler is used to obtain a better air–fuel mixture. Additionally a disc is used to prevent flame flash back. Diameters of the swirler, disc, fuel and air pipes are 66 mm, 125 mm, 35.9 mm, and 144 mm respectively. Although the boiler length is 2300 mm, the water cooling part is 2100 mm as shown in Fig. 3(a). The diameters of the boiler, smoke pipe and stack are 580 mm, 51 mm and 406 mm, respectively. The model of the burner and boiler is shown in Fig. 3(a) and (b). Besides, ignition electrodes are utilized as heat source for the ignition of the gaseous fuel, which works on the principle of the ignition by high-voltage flashover [29]. The ignition electrode and ionization probe are positioned together in front of the burner in the combustion chamber.

The burner and boiler geometries have circular cross section. The number of fuel nozzles is eight with the equal radial angles of 45°. To take advantage of this situation, the full model of the burner and boiler geometries has been divided into 4 equal parts after some modifications to adapt to the periodic boundary condition. The 1/4 geometric model derived from the full model (FM) is considered as a periodic model (PM). The modification was related to assumptions of smoke tube number (FM: 26, PM: 28) and size (PM: Equal diameters), swirl blade number (FM: 13, PM: 12) to decrease the number of mesh and computational time.

Numerical methods and boundary condition

Numerical calculations are carried out by the use of ANSYS Fluent 16 [24], which has a comprehensive application area of CFD, integrated with the NOx post processor. Due to Mach number is smaller than 0.2, at the burner inlets, the density of the species is determined with incompressible ideal gas assumption [30,31]. While the absorption coefficient was selected as 0.5 for the natural gas–hydrogen fuel compositions and 0.45 for the pure hydrogen, scattering coefficients were chosen as 0.01 m^{-1} for these cases [32]. Additionally, wsggm-domain-based was utilized for absorption coefficients of natural gas and methane, while scattering coefficients were taken as 1e-09 for both cases. Velocity inlet is defined for air and fuel boundary conditions based on the mass flow rates of fuel and air. Pressure outlet is defined for the outlet boundary conditions. The experimental and numerical studies utilized under lean conditions ($\phi = 0.833$) condition. The temperatures of inlet air, inlet fuel and boiler wall surface are 291 K, 292 K and 373.65 K, respectively. The thermal load of the burner was taken constant as 1085 kW for all fuel combustions. The steady-state, Reynolds averaged Navier–Stokes equations for mass, momentum, energy and scalar transport are utilized to describe the flow physics.

To use an appropriate radiation model among P1, Rosseland, Discrete Ordinates (DO) and Discrete Transfer (DTRM) models in the problem, optical thickness aL is a good clue. Where a the absorption coefficient and L is length scale of the

Table 1 – Some properties of the simulated fuels at 25 °C.

Fuel	Density (kg m^{-3})	Net heating value (MJ kg^{-1})	Molecular weight (kg $kg\ mol^{-1}$)	Adiabatic flame temperature (K)
Methane	0.667	50.01	16.043	2223 [27]
Natural gas	0.708	49.73	16.989	2233 [28]
Hydrogen	0.081	120	2.016	2370 [27]

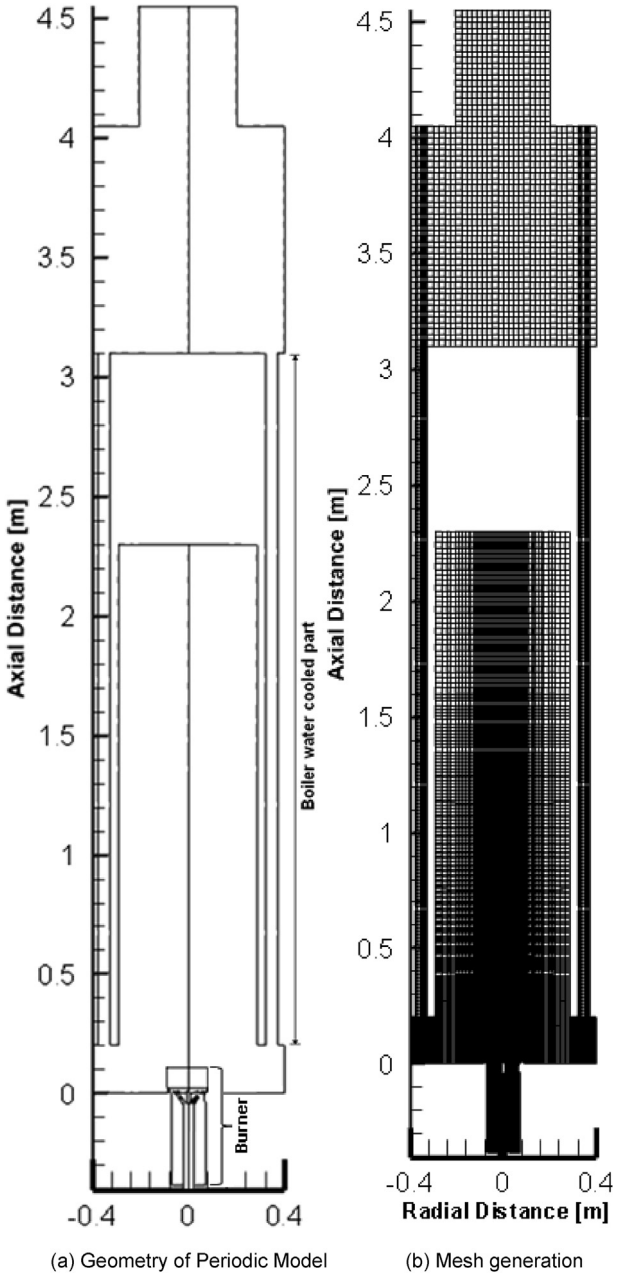


Fig. 3 – Periodic model (a) of the burner and boiler and mesh generation (b).

domain. For flow in a combustor, L is the diameter of the combustion chamber. P1 model is suitable for $aL > 1$, and Rosseland model for $aL \gg 1$ whereas for the optical thin cases ($aL < 1$), only the DTRM and DO models are convenient. Although the use of the DO model requires high computational cost and CPU-intense, it can be preferred among others because of the many advantages such as account for scattering, particulate effect, semi-transparent walls, specular walls, non-gray radiation and localized heat sources [33]. Thus, DO model used for the radiation model in this study ($aL < 1$) may be written as:

$$\nabla\cdot(I(\vec{r},\vec{s})\vec{s}) + (a+\sigma_s)I(\vec{r},\vec{s}) = an^2\frac{\sigma T^4}{\pi} + \frac{\sigma_s}{4\pi}\int_0^{4\pi} I(\vec{r},\vec{s}')\phi(\vec{s},\vec{s}')d\Omega' \quad (1)$$

Large radial pressure gradient occur in the axial and radial direction due to high level of the rotation flow result in distribution of the swirl or rotation in the flow field. This may cause instabilities in the solution process. To use PRESTO! scheme which is well-suited for the steep pressure gradients involved in swirling flows may introduce a solution strategy [33]. Therefore PRESTO! is used for the pressure spatial discretization. Coupled is used as pressure–velocity coupling.

The turbulence flow with significant amount of swirl should be considered using one of the advanced turbulent models such as RNG k–ε model, realizable k–ε model or Reynolds Stress Model (RSM). The convenient choice relies on the importance of the swirl, which can be measured by the swirl number. If the swirl number is less than 0.5 namely moderate swirl, not only realizable k–ε model but also RNG k–ε model are more efficient than standard k–ε model. On the other hand, for highly swirling flow (S > 0.5), RSM is strongly recommended [33]. The performance of a low swirl burner–boiler combustion system with the use of Eddy Dissipation method is determined using RNG and realizable k–ε models. The results have been compared with experimental results in Table 3. It is clear that the result obtained with the realizable k–ε turbulence model proposed for moderate swirl flows show a close similarity, on the other hand, the RNG model show quite different when compared with the experimental result. Because of faster convergence and better results, realizable k–ε turbulence model was used for the turbulence model.

Before starting final analysis, different mesh counts were studied for the mesh sensitivity. The predicted axial temperature and NOx profiles for five different nodes (for PM: 668655, 695374, 725406, and 1144642, for FM: 2674862) are presented in Fig. 4(a) and Table 3. The axial temperatures profiles for the 668655 and 695374 nodes display distinct trends, however, the profiles for 725406, 1144642, 2674862 nodes show approximately same trends. Since increasing the number of nodes to more than 725406 does not create a significant effect on solution, 725406 nodes are used in the analysis.

Table 3 – Mesh independence and turbulent model results.

Polyhedral nodes number	Turbulence model	NOx [ppm]	Geometric model
668655	Realizable	74.64	PM
695374	Realizable	69.61	PM
725406	Realizable	67.38	PM
1144642	Realizable	67.46	PM
2674862	Realizable	67.94	FM
725406	RNG	50.50	PM

Under-relaxation factors were utilized for the control the update of computed variables at each iteration by the pressure-based solver presented in Table 4. The converging criteria for the equations are 10e-05 whereas; it was 10e-06 for energy and radiation and 10e-08 for the NOx prediction emissions.

Table 4 – Under-relaxation factors.

Pressure	0.6
Density	0.25
Body forces	0.95
Momentum	0.4
Turbulent viscosity	0.95
Species concentration	0.95
Energy	0.95
Turbulent kinetic energy	0.75
Turbulent dissipation rate	0.75
Discrete Ordinates [DO]	0.95

Combustion modeling

To deal with the conservation equations for the chemical species, local mass fraction of each species Y_i is anticipated with the use of Fluent through the solution of the convection–diffusion equation for the ith species. The general form of the conservation equations can written as

$$\frac{\partial}{\partial t}(\rho Y_i) + \nabla\cdot(\rho\vec{v}Y_i) = -\nabla\cdot\vec{J}_i + R_i + S_i \quad (2)$$

From Eq. (7), the first term is the rate of the change, the second term is the net rate of flow (convection). Besides, the first term on the right side of the equation is imply the rate of change due to diffusion, where R_i is the net rate of production of species i, by chemical reaction and express the rate of change due to other sources [31,34]. In the turbulent flows with the use of Fluent, the mass fraction is calculated in the following form [31]:

$$\vec{J}_i = -\left(\rho D_{i,m} + \frac{\mu_t}{Sc_t}\right)\nabla Y_i \quad (3)$$

where $D_{i,m}$ is the diffusion coefficient for species i in the mixture, Sc_t is the turbulent Schmidt number and μ_t is the turbulent viscosity, The default value of Sc_t is 0.7.

Species diffusion of the enthalpy has an important effect especially for many multicomponent mixing flows on the flow field and should not be neglected and given by Ref. [31].

$$\nabla\left[\sum_{i=1}^{n} h_i \vec{J}_i\right] \quad (4)$$

The combustion process is extremely complex because of the numerous parameters which are directly or indirectly affect the phenomena. In additional to fuel and oxidizer, sufficient temperature, turbulence and time is required for a good combustion. Besides, some fuels are fast burning, and the overall rate of reaction is controlled by turbulent mixing. The Eddy Dissipation model assumes that the chemical reaction occurs much faster than reactants mixing which is mainly depend on the turbulence. In this approach, the net rate of production of species i due to reaction r, Ri, r, is given by the smaller of the expressions below:

Based on mass fraction of reactants [31]:

$$R_{i,r} = \nu'_{i,r} M_{\omega,i} A \rho \frac{\varepsilon}{k} \min\left(\frac{Y_R}{\nu'_{R,r} M_{\omega,R}}\right) \quad (5)$$

Based on mass fraction of products [31]:

$$R_{i,r} = \nu'_{i,r} M_{\omega,i} AB \rho \frac{\varepsilon}{k} \frac{\sum P Y_P}{\sum_j^N \nu''_{i,r} M_{\omega,j}} \quad (6)$$

here, K turbulence kinetic energy, ε turbulence dissipation rate, Y_P, Y_R mass fraction of species, A Magnussen constant for reactants (default 4.0), B Magnussen constant for products (default 0.5), $M_{\omega,i}$ molecular weight, (R), reactants and (P), products [31].

One of the common point of Eddy dissipation and Eddy break up model of Spalding [35] is the control of the chemical reaction rate which is controlled by the large-eddy mixing time scale (k/ε).

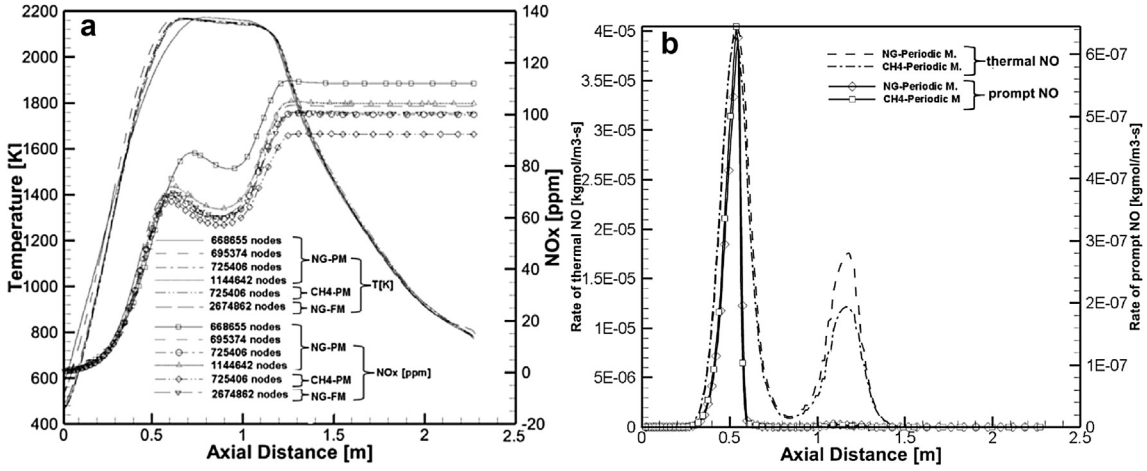


Fig. 4 – Comparison of geometric models and fuel characteristics of natural gas and methane considered the temperature distribution and NOx gradients a) axial temperature and NOx gradients for different nodes number b) axial rate of thermal NO and rate of prompt NO on yz plane.

Species transport, Eddy Dissipation method is used for volumetric combustion model with methane-air-2step reaction mechanism for the methane combustion as follows:

$$CH_4 + 1.5O_2 \rightarrow CO + 2H_2O \quad (7)$$

$$CO + 0.5O_2 \leftrightarrow CO_2 \quad (8)$$

The methane-air-2step reaction mechanism is modified in order to utilize for the natural gas combustion defined as follows:

$$C_{1.058}H_{4.116} + 1.558O_2 \rightarrow 1.058CO + 2.058H_2O \quad (9)$$

$$CO + 0.5O_2 \leftrightarrow CO_2 \quad (10)$$

To model natural gas–hydrogen blending fuels, additional to modified methane-air-2step reaction, one step hydrogen–air reaction mechanism is utilized for the hydrogen combustion defined as:

$$H_2 + 0.5O_2 \rightarrow H_2O \quad (11)$$

Results and discussion

Natural gas (NG) and methane (CH_4) combustion

The natural gas is a mixture which naturally includes such gases as methane, ethane, propane, butane, pentane, hexane, nitrogen, carbon dioxide, oxygen, and hydrogen etc. The compositions and quantities of the natural gas can vary from region to region. The components and mole fractions of the natural gas studied in this study are shown in Fig. 2. As can be seen from the figure, most of the natural gas is methane gas. Therefore, natural gas is modeled as methane with the methane-air-2step reaction mechanism in one side. On the other side, the reaction mechanism is modified (Eq. (9)) for modeling the composition of natural gas taking into account

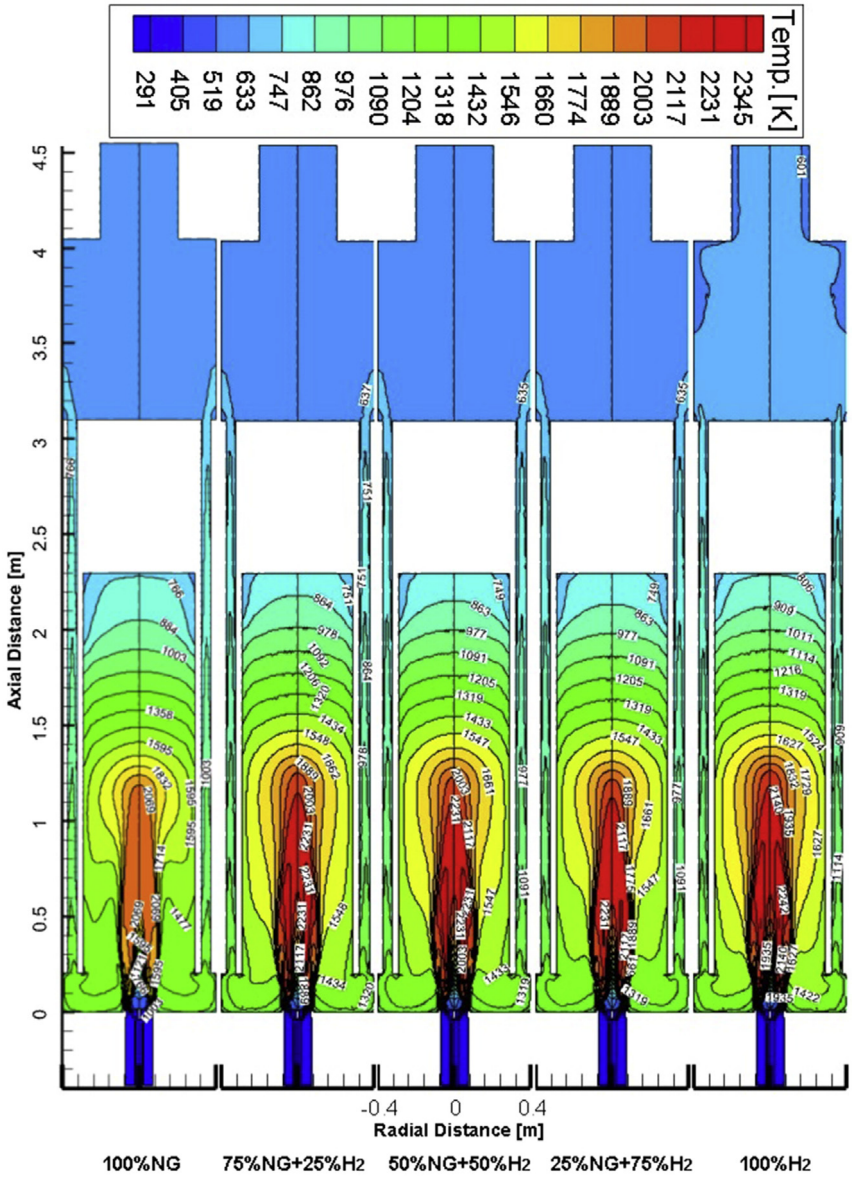


Fig. 5 – The effect of the hydrogen-enriched natural gas combustion on the temperature distribution.

the all species, mixture density, heating value, and molecular weight. In additional to evaluating the combustion characteristics of methane and natural gas, the combustion characteristic of natural gas is investigated with full and periodic models. To evaluate both cases, the results of axial temperature and NOx emission obtained at the center line are given in Fig. 4(a). From the figures, it can be seen that, temperature distribution and NOx gradients for both geometrical models are so close to each other considered the axial temperature and NOx distributions. Additionally, the results of maximum flame temperature (PM: 2173.24 K, FM: 2173.98 K), outlet temperature (PM: 604.26 K, FM: 605.72 K) and outlet NOx (PM: 67.38 ppm, FM: 67.82 ppm) are very similar. Therefore the periodic model can be used instead of full model for the other simulations.

The predicted axial temperatures and NOx emissions distributions of the natural gas and the methane are also presented in Fig. 4(a). It can be seen that the temperatures distributions show the same tendency. However, the maximum flame temperature of the natural gas is slightly higher than the methane flame temperature which results in a deviation of %6 in NOx level. The maximum temperature, outlet temperature and the NOx emissions of the methane combustion is 2171.72 K, 606.75 K, 63.80 ppm, respectively. Besides, NOx gradients of the natural gas and methane show the similar upward trend from 0 m to 0.6 m result from high level of thermal and prompt NO shown in Fig. 4(b). However, NOx emissions of the natural gas and methane at the center line vary slightly especially after 0.6 m where temperature is approximately peaking. From the axial distance of 0.6 m–0.9 m, temperature slightly decreases resulting in reduction of prompt and thermal NO for both fuels. Though temperature still decreases slightly after 0.9 m, NOx level is increase especially due to an increase of short-term thermal NO up to 1.15 m, then temperature drops sharply. However, the NOx maintains its level to the boiler end not only for natural gas but also for methane.

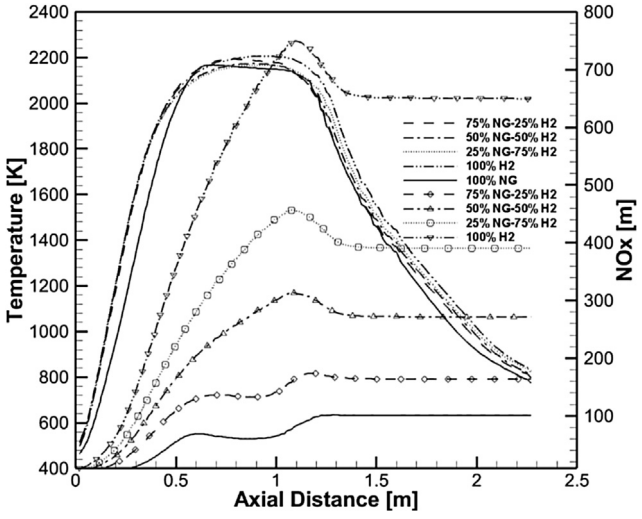


Fig. 6 – The comparison of the natural gas and hydrogen-enriched natural gas axial temperature (shown with lines) and NOx gradients (shown with lines and symbols) distribution at the center line.

Natural gas, hydrogen-enriched natural gas and pure hydrogen combustion

In this study, various amount of hydrogen–natural gas mixtures (thermal load ratio: 100%NG, 75%NG + 25%H_2, 50% NG + 50%H_2, 25%NG + 75%H_2, 100%H_2) were numerically burned at constant burner load (1085 kW) to investigate the effects of hydrogen enrichment on the low swirl burner combustion performance taking into account axial temperature distribution and combustion emissions. Fig. 5 shows the temperature distribution on the yz plane for 100%NG, 75% NG + 25%H_2, 50%NG + 50%H_2, 25%NG + 75%H_2 and 100%H_2 combustion cases. The legend is set to the pure hydrogen combustion results to compare color patterns of all fuel results. From the figure, it can be seen that natural gas flame is placed from the burner head to approximately 1.4 m and the flame diameter is the maximum about at the flame front. The temperature gradually decreases from the flame front to the counter wall. In the figure, the low temperature level is shown when natural gas is burned. It is observed that the

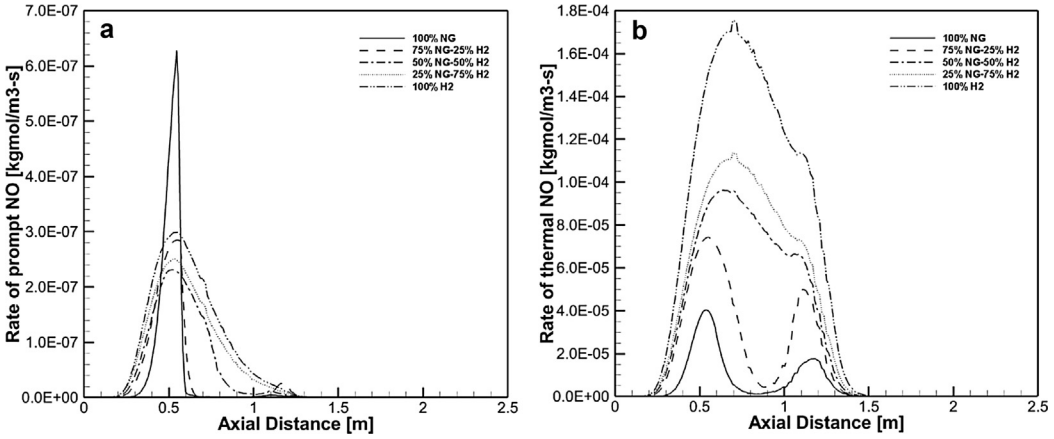


Fig. 7 – The comparison of the natural gas and hydrogen-enriched natural gas a) axial rate of prompt NO distribution, b) axial rate of thermal NO distribution at the center line.

temperature distribution level gradually increased by the addition of hydrogen to natural gas through the flames. In additional to increasing flame length, hydrogen enrichment has also increased the flame diameter of natural gas not only at the burner head but also at the end of the flame length. In spite of increasing the hydrogen ratio in the fuel, the flame lengths and flame diameters changes are limited. The maximum flame and high flame field take place during the pure hydrogen combustion. Fig. 6 gives the axial temperature distribution at the center line of the boiler and burner. It is noticeable that the addition of hydrogen at any rate causes an increase in axial temperature over the range of 0–0.5 m. At the point where the axial distance is 0.6 m, the natural gas combustion reaches the highest temperature value while the hydrogen-enriched natural gas combustions reaches the maximum temperature value about 1 m. Although the temperature level of natural gas combustion decreases slightly after to the peak temperature from 0.6 m to 1.2 m, the increase in temperature levels is still observed with the addition of hydrogen. This situation affects the NOx gradient as shown in Fig. 6. After the 1.2 m of axial distance, temperature levels are sharply decreased to the end of the boiler for all cases. As can be seen from the same figure, the gradual addition of hydrogen to natural gas appears to lead to a gradual increase in the axial temperature levels.

When natural gas, hydrogen-enriched natural gas and pure hydrogen NOx gradient tendencies are evaluated in the axial direction, the NOx emission level increases with hydrogen enrichment (Fig. 6). This is mainly due to high flame temperature of hydrogen result in high rate of thermal NO along the lengths of the flames (0–1.5 m) as shown in Fig. 7(a). The higher amount of hydrogen in the fuel causes the higher the NOx level in case of combustion. For 100% and 75% loadings of natural gas, the NOx increase is two-stage due to increase in thermal and prompt NO at the first stage (0–0.5 m), and an increase in thermal NO at the second stage (1 m–1.2 m). On the other hand, there is a single-stage (0–1.1 m) increase for other gas mixtures and pure hydrogen as shown in Fig. 7(a).

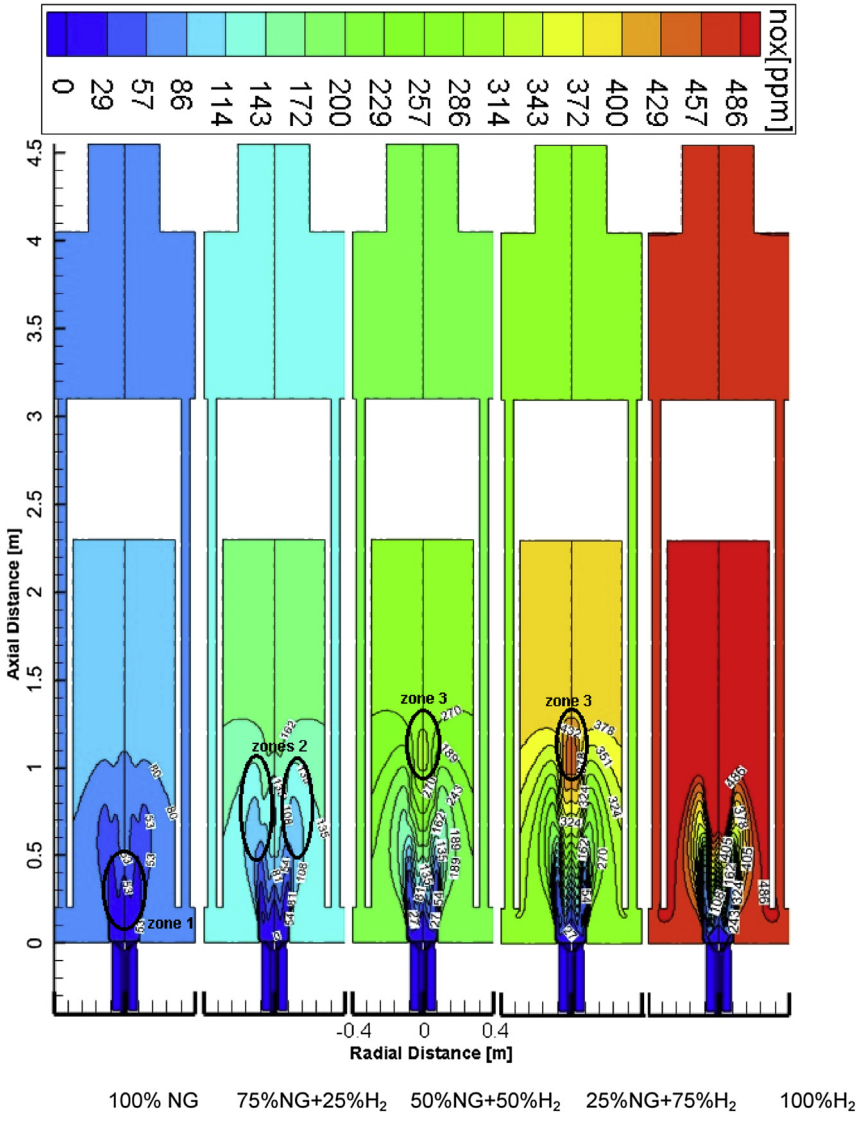


Fig. 8 – The comparison of the NOx emissions of natural gas and hydrogen-enriched natural gas and hydrogen combustions at the yz plane.

After the axial distance of 1.1 m, NOx levels tend to decrease especially for high hydrogen loads (50%, 75% and 100%, respectively) resulted from the depletion of the prompt NO and sharply reduction in the thermal NO. From Fig. 7(a) and (b), it can be seen that the hydrogen-enriched combustion increases the thermal NO and prompt NO. Although during natural gas burning, the rate of prompt NO reaches twice as much as during hydrogen burning, it disappears at a shorter distance. Fig. 8 shows the NOx distribution contours and gives the information about NOx emission generation zones. From the figure, three zones namely zone 1, zone 2 and zone 3 approximately marked. In zone 1, the fuel reaches with swirled air flow results in the prompt NO formation mechanism due to local unburned hydrocarbons. The quantity of NO is relatively high. In zone 2, mostly the outer air coming around disc meets with the rest of fuel in a staged manner. The NO formed in zone 1 as well as molecular N_2 are both oxidized to NO_2 via thermal NOx. In the zone 3, the combustion is generally completed. The concentration of unburned fuels is quite low. In this region, the amount of NO_2 decreases to form NO and N_2 [36]. Especially during the combustion of hydrogen-enriched natural gas at the thermal load ratios of 50%NG + 50%H_2 and 25%NG + 75%H_2, the NO formation is clearly shown by the reduction of NO_2 to NO and N_2 in zone 3. The NOx left in the flue gas limit the final NOx levels which are mainly NO with low quantitative of NO_2.

The addition of hydrogen to natural gas also has an effect on fuel consumption. If natural gas is enriched by hydrogen with 25%, 50% and 75% of thermal load, the amount of consumed fuel is reduced by 14.70%, 29.40% and 44.11%. In case of 100% hydrogen burning instead of natural gas, the amount of fuel reduces by 58.81%.

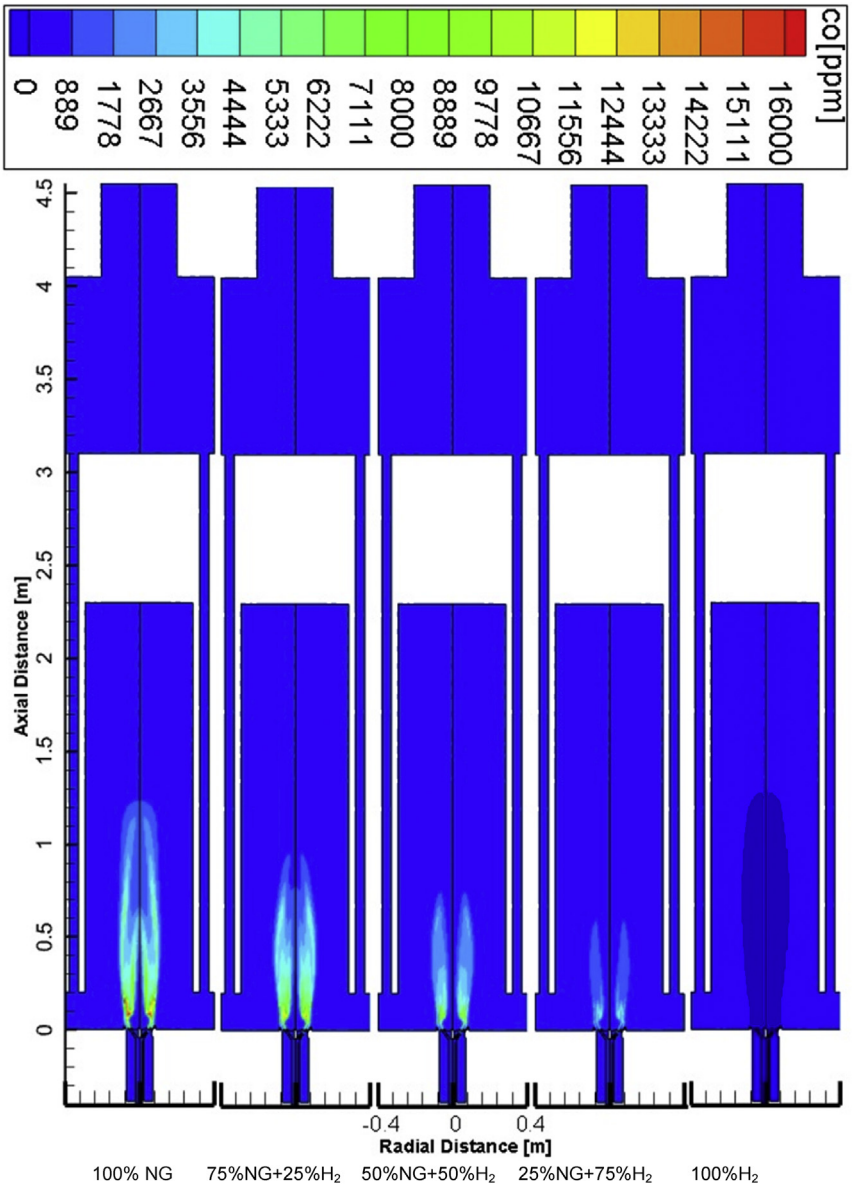


Fig. 9 – The comparison of the CO emissions of natural gas, hydrogen-enriched natural gas and hydrogen combustions at yz plane.

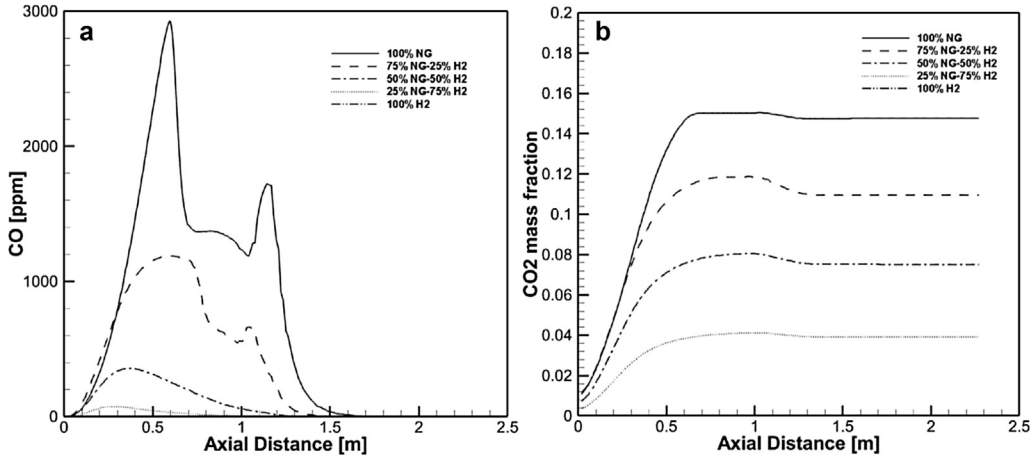


Fig. 10 – The comparison of the natural gas and hydrogen-enriched natural gas a) axial CO distribution, b) CO_2 distribution at the center line.

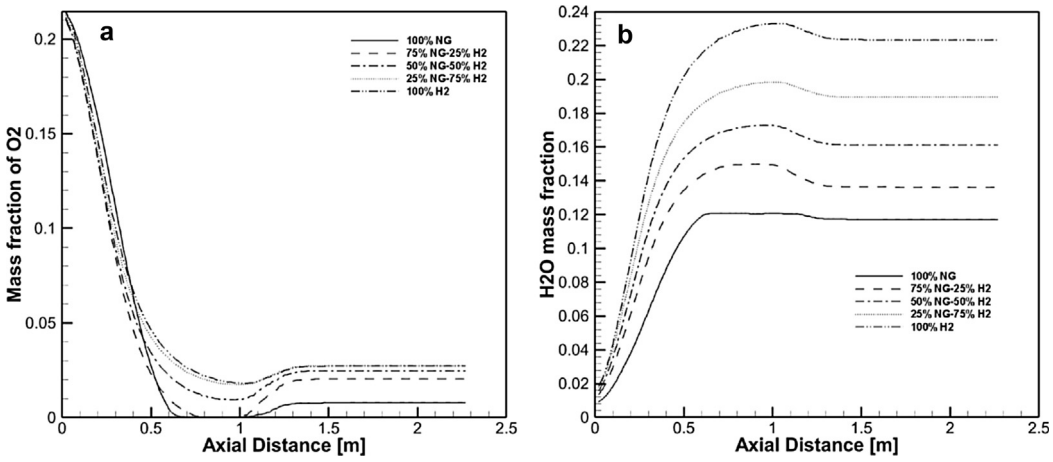


Fig. 11 – The comparison of the natural gas and hydrogen-enriched natural gas a) axial O_2 distribution at the center line, b) axial H_2O distribution.

CO, CO_2, H_2O, O_2, CH_4 and H_2 combustion species

From the simulation results based on natural gas, hydrogen-enriched natural gas and hydrogen fuels combustion, CO gradients distributions contours and axial direction values at center lines are shown in Figs. 9 and 10, respectively. It is clearly shown from in the both figures that, hydrogen addition on natural gas decrease the level of CO, precisely reduce it to zero when pure hydrogen is utilized instead of natural gas. Although the CO levels inside the boiler too high especially for carbon (C) based fuels such as natural gas and hydrogen-enriched natural gas, the values at the center line are quite low especially at the boiler outlet (0 ppm). It is also demonstrated in Fig. 10(a) that the combustion of the high hydrogen-enriched natural gas (%25NG + 75%H_2) gives less CO level compared to the low hydrogen-enriched load (%75NG + 25% H_2). CO_2 combustion emissions also show the same tendency with CO emissions and decrease with increasing hydrogen load in the fuel mixtures, eventually dropping to zero with pure hydrogen burning as shown in Fig. 10(b). Besides, reducing the natural gas load by half almost resulted in the reduction of CO_2 emissions by half.

Contrary to CO and CO_2 emissions, the H_2O value is particularly high in products of hydrogen-enriched natural gas combustions. Since only the product of the hydrogen oxidizer combustion is H_2O. Furthermore, the level of H_2O almost doubles as shown in Fig. 11(a), when hydrogen is burned as fuel instead of natural gas.

The distribution of the O_2, which is one of the most important species of the combustion known as an oxidizer, in the boiler is presented in Fig. 11(b). From the figures, when burning begins in the first part of the boiler, hydrogen-enriched fuels react with more oxygen. In addition, when combustion is developed and completed, the amount of excess oxygen remaining in the boiler increases with increasing hydrogen mass fraction.

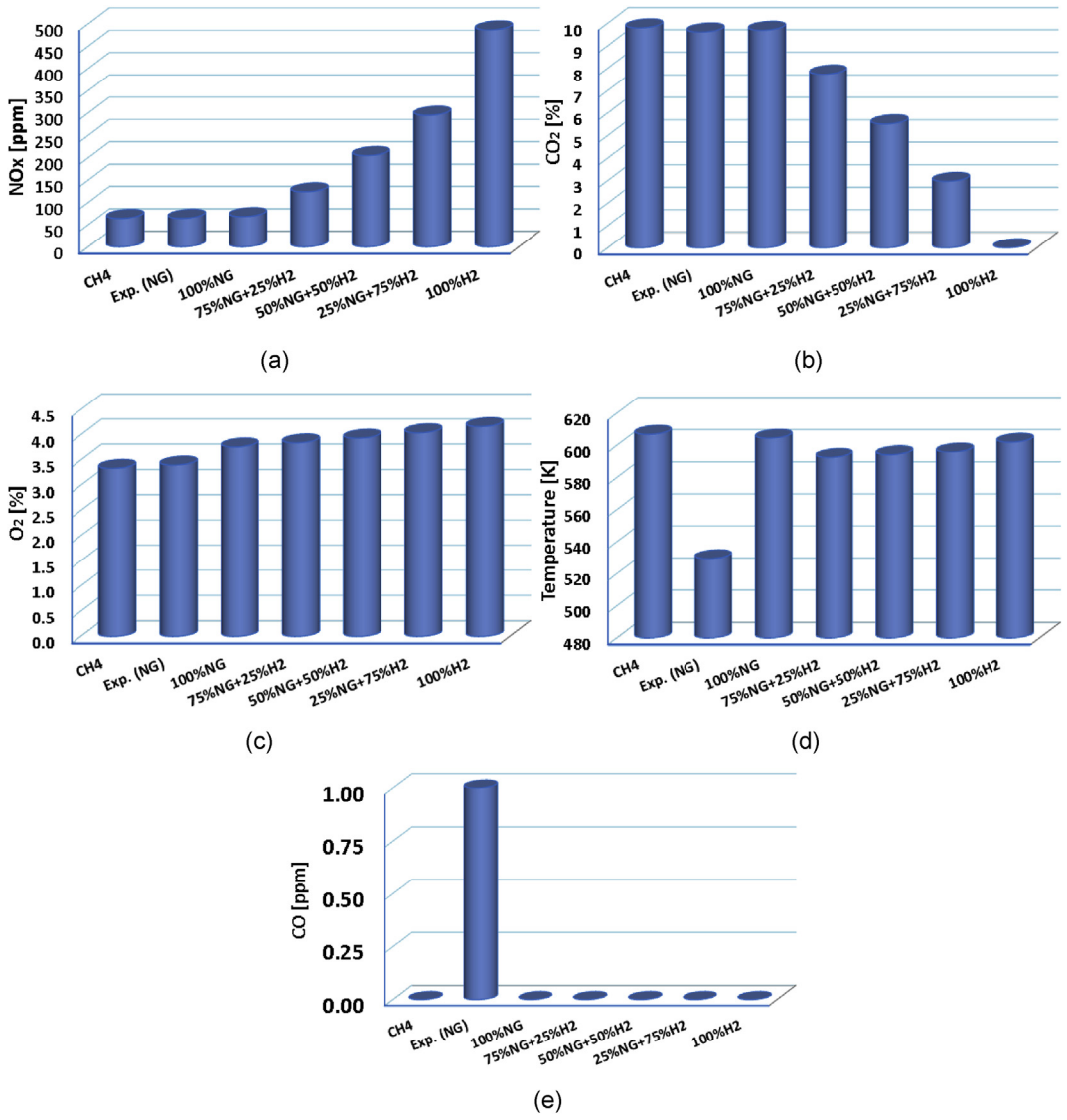


Fig. 12 – The comparison of the combustion products and outlet temperature (T_{out}) of studied fuels a) NOx emissions, (b) CO_2 emissions (c) O_2 species (d) T_{out} measurement (e) CO emissions at the boiler outlet (stack inlet).

Combustion emissions at the outlet

In order to compare the experimental and CFD results, combustion emissions and temperature at the outlet have compared in Fig. 12. Although the combustion emissions such as NOx and CO_2 of NG and CH_4 close to each other, they show a slight deviation as shown in Fig. 12(a), (b). However, the deviation of O_2 and outlet temperatures (T_{out}) is greater (see Fig. 12(c), (d)). When the natural gas experimental test results are taken as a reference, the deviations in CFD results for NOx, CO_2, CO and T_{out} in NG combustion are 6.16%, 0.86%, 10.51% and 14.15%, respectively. In addition, the deviations in CFD results for NOx, CO_2, CO and T_{out} in CH_4 combustion are 0.31%, 1.96%, 1.93% and 14.61%, respectively. CFD results of natural gas and methane combustion productions are similar to each other but O_2. The difference between O_2 concentrations for two fuels is around 8.58%. On the other hand, the combustion emissions of the hydrogen-blending natural gas and pure hydrogen show quite differences as compared NG. When hydrogen add to the natural gas loadly by 25%, 50% and 75% and utilize instead of natural gas by 100%, the predicted NOx levels increase by 92.81%, 219.72%, 360% and 659.30%, respectively. Additionally the quantities of CO_2 are remarkably decreased by 19.45%, 42.58%, 69.15% and 100%, respectively. Furthermore, the O_2 concentrations are increased by 12.91%, 15.64%, 18.78% and 22.43%, respectively. The predicted gases temperatures levels at the boiler outlet are shown in Fig. 12(d). The predicted temperatures of the combustion gases of CH_4 and NG are close to each other and higher than pure hydrogen and hydrogen-blended natural gas combustions. On the other hand, the boiler gas outlet temperature increases as the hydrogen ratio in the fuel increases. The predicted emission value of CO was approximately 0 ppm for all fuels while the measured level was 1 ppm during the natural gas combustion as shown in Fig. 12(e). It is understood from the results that modeling natural gas as methane or

natural gas gives approximately results based on the predictions level of NOx, CO_2, CO maybe O_2 but involves some deviation especially for temperature guess at the outlet of the boiler. Additionally, with the addition of hydrogen on the natural gas, the quantities of CO_2 are remarkably decreased at the outlet. Furthermore, when pure hydrogen used instead of natural gas, CO_2 is disappeared due to absence of carbon element in the hydrogen fuel. Unlike CO_2, NOx increases as the ratio of hydrogen in the natural gas increases result from high flame temperatures. And also when pure hydrogen is burned, NOx emissions increase significantly due to highest flame temperature.

Conclusion

Experimental results obtained from natural gas combustion in a low swirl burner and hot water boiler have been used as boundary conditions for two geometrical models for CFD modeling. One of the two models is based on a periodic boundary condition, which allows working with fewer meshes instead of a dense mesh. Then, combustion characteristics and emissions of the methane, which is the main component of natural gas and correspond to the majority, (95.05%) have examined with the methane-air-2step reaction mechanism. Additionally, the CH_4 reaction mechanism has been modified to take into account natural gas properties. In this way, the emissions levels of both fuels are revealed. Further, the effects of hydrogen-enriched natural gas and pure hydrogen on the combustion characteristics of the burner–boiler have been investigated at the same thermal load (1085 kW). The results are compared to the natural gas combustion results. The conclusions arising from this study are as follows:

- From the obtained results, the realizable k–ε model is more suitable than the RNG model for the prediction of NOx emission of low swirl turbulent flows.
- Modification of the unimportant parts of the geometric model in order to use periodic boundary condition gives satisfactory results without going out of working conditions.
- With the use of Eddy Dissipation combustion model, natural gas can be modeled with methane-air-2step reaction mechanism with some deviation. However, it is more realistic approach to modify methane reaction mechanism taking into consideration the species, mixture density, heating value and molecular weight of natural gas.
- Combustion behaviors of natural gas (with modified reaction mechanism) and methane (with methane-air-2step) are similar and the results are close to each other. However, NOx and oxygen levels show differences. The deviation between NOx levels is 6% while the oxygen levels are 11%.
- In the case of natural gas–hydrogen mixtures, when hydrogen addition to the natural gas by 25%, 50% and 75%, the NOx emission level increases by 92.81%, 219.72% and 360% respectively.
- Since there is no C element in pure hydrogen fuel, CO and CO2 emissions do not occur in the case of hydrogen combustion, but NOx gives the highest level with 485.95 ppm. In this case, the NOx emissions at the boiler output increase by 659.30% compared to pure natural gas.
- Although the prompt NO formed during natural gas combustion is higher than the NO generated during hydrogen combustion, the NO formed in a larger region during hydrogen combustion.
- The addition of hydrogen to natural gas also has an effect on fuel consumption. If natural gas is enriched by hydrogen with 25%, 50% and 75%, the amount of consumed fuel is reduced by 14.70%, 29.40% and 44.11% for the same burner capacity. In case of 100% hydrogen burning instead of natural gas, the amount of fuel reduces by 58.81%.

Acknowledgment

This academic research supported by Yildiz Technopark and Company of Termo-Heat Isı San. A.Ş. We gratefully thank to the management and employees of the both companies for their supports.

REFERENCES

[1] http://www.ghgonline.org/otherco.htm.
[2] Yilmaz T, Yilmaz A, Erdinç MT. Energy recovery from hydrogen combustion at elevated pressures. Int J Hydrogen Energy 2017;42(36):23361–5.
[3] Sandalcı T, Karagöz Y. Experimental investigation of the combustion characteristics, emissions and performance of hydrogen port fuel injection in a diesel engine. Int J Hydrogen Energy 2014;39:18480–9.
[4] Wu W, Wang B, Shi W, Li X. Absorption heating technologies: a review and perspective. Appl Energy 2014;130:51–71.
[5] Hammond GP, Norman JB. Heat recovery opportunities in UK industry. Appl Energy 2014;116:387–97.
[6] Mokheimer EMA, Sanusi YS, Habib MA. Numerical study of hydrogen-enriched methane-air combustion under ultra-lean conditions. Int J Hydrogen Energy 2016;40:743–62.
[7] Colella WG, Jacobson MZ, Golden DM. Switching to a U.S. hydrogen fuel cell vehicle fleet: the resultant change in emissions, energy use, and greenhouse gases. J Power Sources 2005;150:150–81.
[8] Michalovic M. "Beyond hydrogen", (The new chemistry of fuel cells). Chemmatters December 2007:17–9. Teacher's guide.
[9] Kahveci EE, Taymaz I. Experimental investigation on water and heat management in a PEM fuel cell using response surface methodology. Int J Hydrogen Energy 2014;39:10655–63.
[10] Mishra DP. Fundamentals of combustion, revised edition. New Delhi-110001: PHI Learning Private Limited; 2010.
[11] Sharma S, Ghoshal SK. Hydrogen the future transportation fuel: from production to applications. Renew Sustain Energy Rev 2015;43:1151–8.
[12] Riis T, Hagen Elisabet F, Vie PJS, Ulleberg Øystein. Hydrogen production R&D: priorities and gaps. IEA Hydrogen Implementing Agreement (HIA). 2006.
[13] Yılmaz I, Ilbas M. An experimental study on hydrogen-methane mixtured fuels. Int Commun Heat Mass Transf 2008;35:178–87.
[14] Ilbas M, Yılmaz I. Experimental analysis of the effects of hydrogen addition on methane combustion. Int J Energy Res 2012;36:643–7.

[15] Yılmaz I, Taştan M, Ilbas M, Tarhan C. Effect of turbulence and radiation models on combustion characteristics in propane–hydrogen diffusion flames. Energy Convers Manag 2013;72:179–86.
[16] Bouras F, Attia MEH, Khaldi F, Si-Ameur M. Control of methane flame properties by hydrogen fuel addition: application to power plant combustion chamber. Int J Hydrogen Energy 2017:1–8. http://dx.doi.org/10.1016/j.ijhydene.2016.11.146.
[17] Haj Ayed A, Kusterer K, Funke HHW, Keinz J, Striegan C, Bohn D. Experimental and numerical investigations of the dry-low-NOx hydrogen micromix combustion chamber of an industrial gas turbine. Propul Power Res 2015;4:123–31.
[18] Haj Ayed A, Kusterer K, Funke HHW, Keinz J, Bohn D. CFD based exploration of the dry-low-NOx hydrogen micromix combustion technology at increased energy densities. Propul Power Res 2017. http://dx.doi.org/10.1016/j.jppr.2017.01.005.
[19] Coppens FHV, Konnov AA. The effects of enrichment by H_2 on propagation speeds in adiabatic flat and cellular premixed flames of $CH_4 + O_2 + CO_2$. Fuel 2008;87:2866–70.
[20] Schefer RW. Combustion of hydrogen-enriched methane in a lean premixed swirl burner. Proc Combust Inst 2002;29:843–51.
[21] Ouimette P, Seers P. NOx emission characteristics of partially premixed laminar flames of $H_2/CO/CO_2$ mixtures. Int J Hydrogen Energy 2009;34:9603–10.
[22] Dutka M, Ditaranto M, Løvås T. NOx emissions and turbulent flow field in a partially premixed bluff body burner with CH_4 and H_2 fuels. Int J Hydrogen Energy 2016;41:12397–410.
[23] Cellek MS, Engin T. 3-d Numerical investigation and optimization of centrifugal slurry pump using computational fluid dynamics. J Therm Sci Technol 2016;36:69–83.
[24] ANSYS® Academic Research, Release 16.
[25] Termo-Heat Isı San. A.Ş. http://www.termo-heat.com.
[26] ÇORDAŞ Çorlu Natural Gas Distribution Corporation, 2016.
[27] Levis B, Von Elbe G. Combustion, flames and explosions of gases. 3rd ed. New York: Academic Press; 1987.
[28] Reed Richard J. North American combustion handbook: a basic reference on the art and science of industrial heating with gaseous and liquid fuels. 3rd ed., vol. 1; 1985.
[29] http://www.thermaco.co.uk/electrodes.php, 25.11.2016.
[30] Colorado A, McDonell V. Prediction of NOx emissions from premixed natural gas and hydrogen enriched flames stabilized with a low–swirl burner. The fall 2013 Technical meeting of the western states section of the combustion institute hosted at Colorado State University in fort Collins, Colorado on October 7–8, 2013.
[31] ANSYS Fluent Theory Guide, Release 16.
[32] Ilbas M. The effect of thermal radiation and radiation models on hydrogen hydrocarbon combustion modelling. Int J Hydrogen Energy 2005;30:1113–26.
[33] Inc Fluent. Fluent 6.2 user guide. January, 2005.
[34] Bakker A. Modeling chemical reactions with CFD. Reactin flows-lecture 10. http://www.bakker.org/dartmouth06/engs199/10-react.pdf.
[35] Spalding DB. Mixing and chemical reaction in steady confined turbulent flames. In: 13th symp. (Int'l.) on combustion. The Combustion Institute; 1970.
[36] Barendregt S, Risseeuw l, Waterreus F. Applying ultra-low-NOx-burners. Petrochem Gas Process 2006. PTQ Q2 2006, 1-6.